

# Optimal Joint TDPA Formulation for Kinematically Redundant Robot Manipulators

Francesco Porcini<sup>1</sup>, Massimiliano Solazzi<sup>1</sup> and Antonio Frisoli<sup>1</sup>

**Abstract**—The accomplishment of a successful teleoperation task requires guaranteeing system stability and transparency. Communication delay (in particular variable time delay), quantization and discretization negatively affect system stability and might be overcome with Time Domain Passivity Approach (TDPA), a model-free and robust way to cope with energy injection due to communication delay. However, this method degrades the transparency of the teleoperation system and worsens tracking performance, introducing in particular position drift error at the slave side and high frequency vibration (jittering) at the master side. In this work, we propose a new joint passivity controller formulation for kinematically redundant manipulators. Our approach stabilizes the system guaranteeing minimal performance loss by privileging the dissipation of the observed energy in the Jacobian null-space. The residual energy (if any) is dissipated in an orthogonal subspace. This is achieved by the solution of an optimization problem with appropriately defined cost functions and constrained to dissipate the energy observed by the passivity observer, guaranteeing the stability of the system. The effectiveness of our algorithm is tested in simulation with both constant and variable time delays.

## I. INTRODUCTION

A teleoperation system allows the user to control a robot interacting with a remote environment. In general, it is composed of a master (a haptic device driven by the user) and a slave (a robotic device that interacts with the remote environment) connected through a communication channel, which allows the information exchange. The choice of the architecture determines the physical information that must be transmitted over the communication channel [1], [2].

During a teleoperation task, precise master position tracking by the slave and clear force feedback signal increase dexterity and intuitiveness, and they constitute a benchmark for the architecture transparency. Stability and transparency are the most important requirements of a teleoperation system; they are concurrent features and stability should be preferred for safety reasons. However, stability is deteriorated by phenomena like quantization, sampling, and time delay. In particular, the last one is the main source of instability as it makes the communication channel exhibit an active behaviour. Different methods have been developed to ensure stability [3], [4], [5]. Among these, the *Time Domain Passivity Approach (TDPA)* guarantees the stability passivating the system in the time domain [6], [7], [8], by identifying the elements of the architecture that exhibit an active behaviour and dissipating energy through a virtual time-dependent damper. Originally developed for *1-degree*

*of freedom (1-DoF)* systems, the TDPA was extended to *n-degrees of freedom (n-DoFs)* systems with formulations in the Cartesian space [9], [10], [11], [12], but there is an almost total absence of joint space formulations. Moreover, most works focus on architectures in which master and slave are kinematically symmetrical, greatly limiting development.

The TDPA guarantees stability (even in presence of variable time delay [13]) at the cost of position drift error at the slave side [14] and rendered force high frequency vibrations (jittering) at the master side [15], thus leading to a degradation of transparency. Minimizing the drift error and providing the user with clean force feedback is fundamental in complex and critical tasks such as in disaster response ones [16]. On the slave side, many drift compensation methods have been proposed through the years [14], [17], [18], but they only work while the system is passive making the drift recovery slow and inefficient especially for high dissipated energies. This is a still open problem that degrades the performance of any passivated teleoperation architecture. On the master side, few works were proposed to minimize the high-frequency vibrations that occur as an effect of the stabilizing action. Among them, Ryu et al. proposed in [13] a virtual mass and spring (VMS) system on the master side acting as a kind of low-pass filter, but this method suffers from references distortion (even greater in presence of variable time delay) and requires a set-up dependent tuning of the parameters. In [15], a novel approach named Observer-Based Gradient Controller was proposed to address this problem, but even if the vibrations decrease significantly, a perfect fidelity of the force to render is not guaranteed. Both drift error on the slave side and force jittering on the master side are caused by the stabilizing action of the *PC* exploited on the *task space*.

For a redundant manipulator, an efficient dissipation strategy may involve the *null-space* (or *self-motion space*), since movements performed in this space do not affect the task space. In [19], it was proposed the idea of *subspace oriented* dissipation: it consists in privileging the dissipation in the Jacobian null-space, thus the task space is less affected (up to none) by the stabilizing action. This work has paved the way for interesting applications (for example in aerospace robotics [20]). However, this case of study is limited to impedance-based devices and the presented damping elements are assumed to be limited on the base of the sampling time. Moreover, this limit does not take into account the manipulator configuration, while power-limited actuators require an on-line solution of a quadratic programming (QP) problem in order to not exceed power limitations. Furthermore, this algorithm was not tested on

<sup>1</sup>Scuola Superiore Sant'Anna, IIM Institute, PERCRO Laboratory, Pisa, Italy, francesco.porcini@santannapisa.it



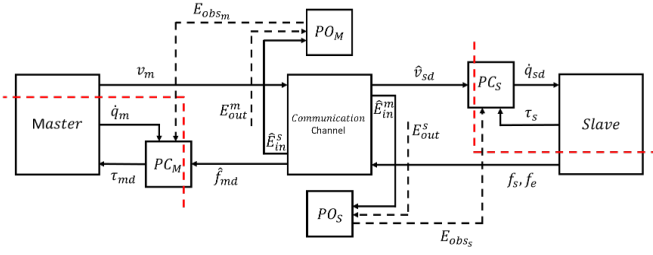


Fig. 2: *Position-Force* teleoperation architecture in the mixed Cartesian-joint domain. The master transmits the Cartesian velocity as reference, while likewise the slave transmits the force. Both these quantities are used to compute the energies by the *POs* in the Cartesian domain. The *PCs* are responsible for reporting the Cartesian reference in the joint space and for applying the dissipating action directly at joint level.

or as a damping factor that multiplies the inertia matrix of the manipulator transposed in Cartesian coordinates. All the damping factors are computed on the base of the energy observed.

### III. TIME DOMAIN PASSIVITY APPROACH WITH KINEMATIC REDUNDANCY

In this section, it is presented a new joint passivity controller formulation that exploits the kinematic redundancy of a robotic manipulator to optimally stabilize the system and minimizes the dissipation effect in the task space. For a multi-DoFs system, a strategy to distribute the energy observed by a *PO* among the degrees of freedom is required. A valid approach consists in projecting the dissipation action in the Jacobian null-space, resulting in a task space untouched by the dissipating action. Such a strategy is intuitively easy to be implemented directly in the joint space. However, there are no such joints formulations in the *state-of-the-art*. This may be due to the fact that a joint formulation may be supposed to require that data transmitted over the communication channel are joint space variables. It is easily understood that this way of transmitting data requires a new definition of the *POs* among with a full kinematic symmetry between the master and slave, greatly limiting the applicability of a joint passivation strategy. However, it is possible to implement a mixed-spaces architecture in which the transmitted data belong to the Cartesian space (see figure 2 for a generic *PF* architecture). This makes possible not to change the *PO* definition (in fact, energy is an invariant scalar quantity) and does not require kinematic symmetry between master and slave. In such an architecture the *PC* will perform the dissipation action at joint level.

Consider a slave (*s* subscript) and a master (*m* subscript) redundant robot manipulators with  $n_s, n_m$  degrees of freedom in an  $m$ -dimensional work-space (thus the redundancy is given by  $r_s = n_s - m$  and  $r_m = n_m - m$ ). The redundant joint formulation of the *PC* (*rPC*) can be derived by analogy with the Cartesian one (*cPC*): at joint level, the *passivated velocity* (or *passivated force*) must equal the *non-passivated velocity* (or *non-passivated force*) plus a *dissipation vector*.

$$\begin{aligned} \dot{\mathbf{q}}_{sd}(k) &= \hat{\mathbf{q}}_{sd}(k) + \mathbf{d}_s(k) \\ \boldsymbol{\tau}_{md}(k) &= \hat{\boldsymbol{\tau}}_{md}(k) + \mathbf{d}_m(k) \end{aligned} \quad (5)$$

where  $\hat{\mathbf{q}}_{sd}(k) = J_s^+ \hat{\mathbf{v}}_{sd}$  (with  $J_s \in \mathbb{R}^{m \times n_s}$  and  $J_s^+ = J_s^T (J_s J_s^T)^{-1}$  right pseudo-inverse of the slave Jacobian matrix) and  $\hat{\boldsymbol{\tau}}_{md}(k) = J_m^T \hat{\mathbf{f}}_{md}$  (with  $J_m \in \mathbb{R}^{m \times n_m}$  is the master Jacobian matrix). The *POs* compute the scalar power  $w_s(k)$  and  $w_m(k)$  that the controllers must dissipate to guarantee stability. To lighten the notation, the time  $k$  dependence will be omitted from now on.

#### A. Admittance-based Formulation

The problem is defined and solved using the optimum Lagrange method. To guarantee stability, the *rPC* must be constrained to dissipate the observed energy  $w_s$  into the Jacobian null-space. The imposed constraint is scalar, this means that we need a cost function to find the remaining  $n_s - 1$  components of the dissipation vector. The best cost function to reduce the load on the actuators is a function that minimizes the norm of the dissipation vector:

$$\begin{cases} \dot{\mathbf{q}}_{sd} = \hat{\mathbf{q}}_{sd} + \underbrace{P_s \mathbf{d}_1}_{\mathbf{d}_s} \\ \boldsymbol{\tau}_s^T P_s \mathbf{d}_1 + w_s = 0 \rightarrow \text{constraint} \\ g(\mathbf{d}_1) = \frac{1}{2} \mathbf{d}_1^T \mathbf{d}_1 \rightarrow \text{cost function} \Rightarrow \underset{\mathbf{d}_1}{\text{argmin}} \{g(\mathbf{d}_1)\} \end{cases} \quad (6)$$

where  $P_s = I - J_s^+ J_s \in \mathbb{R}^{n_s \times n_s}$  is the slave's Jacobian null-space projector and  $I \in \mathbb{R}^{n_s \times n_s}$  is the identity matrix. For this problem, the solution is the following:

$$\mathbf{d}_s = \alpha_s P_s \boldsymbol{\tau}_s \quad \text{with} \quad \alpha_s = \frac{-w_s}{\boldsymbol{\tau}_s^T P_s \boldsymbol{\tau}_s} \quad (7)$$

where  $\alpha_s$  is the damping element of the controller. It is straightforward to verify that the solution always verifies the constraint on the power ( $\boldsymbol{\tau}_s^T P_s \mathbf{d}_s = w_s$ ).

1) *Power-limited Actuators*: Equation 7 attempts to dissipate the overall observed power in the Jacobian null-space. This is possible in case of unlimited dissipating capability. However, the dissipating capability of a robot depends reasonably on the actual configuration and on the power limits of its actuators, preventing from dissipating all the power in the Jacobian null-space. In fact, consider without losing generality  $n_s = 2$  and  $m = 1$  (thus  $r_s = 1$ ). Referring to figure 3, consider three example linear constraints, each associated to an observed energy  $w_i$ , so that the following holds:

$$\begin{aligned} \sigma_i : \boldsymbol{\tau}_s^T P_s \mathbf{d}_s - w_i &= 0 \quad \text{with} \quad i = 1, 2, 3 \\ w_{1s} &< w_{2s} < w_{3s} \end{aligned} \quad (8)$$

According to the manipulator joint limits, it is possible to define a maximum joint speed vector  $\hat{\mathbf{q}}_{MAX_s}$ . Thus, in a certain configuration the maximum speed performable in the Jacobian null-space is  $P_s \hat{\mathbf{q}}_{MAX_s}$ . Since the joint dissipation vector  $\mathbf{d}_s$  is a joint speed, it must remain in the circumference limited by  $\|P_s \hat{\mathbf{q}}_{MAX_s}\|$ . The constraint is verified if the Jacobian null-space projected torque, scaled by the damping

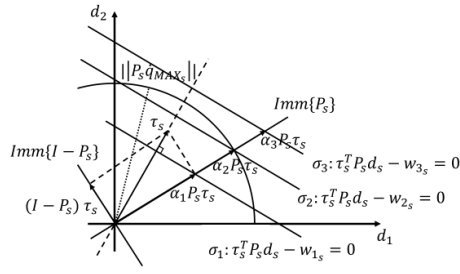


Fig. 3: Joint space representation for an admittance-based manipulator with  $n_s = 2$ ,  $m = 1$  and  $r_s = 1$ . A certain power can be dissipated in the Jacobian null-space according to the maximum displayable joint speed in such a space.

element, intercepts the constraint line inside the radius of the circumference. In the example, this is possible for powers  $w_{s1}$  and  $w_{s2}$  (at limit), but power  $w_{s3}$  would require not dispensable joint speed. Thus, the following two points must be addressed:

- It is necessary to dissipate the remaining power (if any) in another subspace to guarantee stability.
- The damping element must be constrained taking into account the power-limited actuators.

2) *Null-space Orthogonal Dissipation*: The Jacobian null-space defines a privileged dissipation direction (or subspace). However, if (and only if) the privileged dissipating action exceeds the power limits it is necessary to define a secondary dissipating action that dissipates the residual energy guaranteeing stability defining a dissipation priority logic. When required, the secondary action should not introduce disturbance components in the privileged direction, otherwise this will result in altering the optimality or the feasibility of the solution. For example, consider a generic  $\mathbb{R}^2$  space in which the dissipation takes place (see figure 4) with a privileged dissipation direction  $\hat{\mathbf{d}}_p$  and its orthogonal  $\hat{\mathbf{d}}_o$ . Moreover, we define a vector  $\mathbf{v}$  (versor  $\hat{\mathbf{v}}$ ) so that  $\mathbf{v}^T \mathbf{d} = w$ . Assume that the power to be dissipated requires the privileged dissipation to reach its maximum  $\mathbf{d}_{pM}$ . Consider two possible dissipations:  $\mathbf{d}_1 = \mathbf{d}_{pM} + \mathbf{d}_{r1}$  (with  $\mathbf{d}_{r1} \perp \hat{\mathbf{d}}_o$ ) and  $\mathbf{d}_2 = \mathbf{d}_{pM} + \mathbf{d}_{r2}$  (with  $\mathbf{d}_{r2} \not\perp \hat{\mathbf{d}}_o$ ). Thus, the following holds:

$$\begin{aligned} \mathbf{d}_1 = \mathbf{d}_{pM} + \mathbf{d}_{r1} &\Rightarrow \mathbf{v}^T \mathbf{d}_1 = \underbrace{[\mathbf{v}^T \mathbf{d}_{pM}]}_{w_p} + \underbrace{[\mathbf{v}^T \mathbf{d}_{r1}]}_{w_o} \\ \mathbf{d}_2 = \mathbf{d}_{pM} + \mathbf{d}_{r2} &= \mathbf{d}_{pM} + (\mathbf{d}_{ro2} + \mathbf{d}_{rp2}) \\ &\Rightarrow \mathbf{v}^T \mathbf{d}_2 = \underbrace{[\mathbf{v}^T (\mathbf{d}_{pM} + \mathbf{d}_{rp2})]}_{w_p} + \underbrace{[\mathbf{v}^T \mathbf{d}_{ro2}]}_{w_o} \end{aligned} \quad (9)$$

where  $w_p$  is the power dissipated in the privileged direction, while  $w_o$  is the power dissipated in its orthogonal. Thanks to the orthogonality of the subspaces, the overall dissipated power is the sum of the two terms. The priority dissipation algorithm produces  $\mathbf{d}_{pM}$  as first vector, then, if  $\mathbf{d}_{r2}$  is summed, its component in the preferred direction ( $\mathbf{d}_{rp2}$ ) leads to a dissipated power in the privileged subspace higher (figure 4a) or lower (figure 4b) with respect the

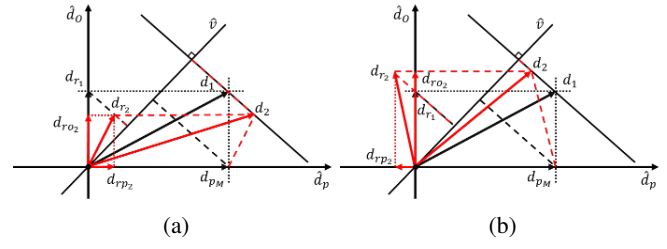


Fig. 4: Graphical representation of the dissipation space. (a-b) represent different cases in which the residual dissipation vector ( $\mathbf{d}_{r2}$ ) is not orthogonal with respect the privileged dissipation direction ( $\hat{\mathbf{d}}_p$ ). In both figures, the represented case is compared with a residual dissipation vector ( $\mathbf{d}_{r1}$ ) orthogonal to  $\hat{\mathbf{d}}_p$ . Different components of vectors in the three cases dissipate the same power.

one that the manipulator is able to display. In the first case the solution leads potentially to instability, while in the other case the capabilities of the manipulator are not fully exploited. In conclusion, in a priority dissipation logic, the best direction (or subspace) to dissipate the residual power is orthogonal to the privileged direction. In this way, if the privileged dissipation reaches its limit, the residual dissipation performs its action without compromising the first one. These considerations hold regardless of the space in which the dissipation is performed, whether it is Cartesian or at the joint space and it was not taken into account by other methods presented in literature.

3) *Complete Admittance-based Formulation*: The dissipating vector can be thought as the sum of two terms, one (privileged) in the Jacobian null-space ( $N$ ) and the remaining (or residual) energy in the Jacobian null-space orthogonal subspace ( $O$ ). Each of these is characterized by its damping element. Since the formulation is expressed at the joint level, each damping element will be limited linking the dissipation vector to the manipulator joint power limits in each subspace. The priority dissipation strategy and the orthogonality make possible to design the two components of the damping vector separately. Moreover, it is straightforward that the overall dissipated energy is given by the sum of the dissipated energies by the two individual components of the dissipating vector. Thus, the admittance formulation of the *rTDPA PC* can be formulated as follows:

$$\hat{\mathbf{q}}_{sd} = \hat{\mathbf{q}}_s + \mathbf{d}_s \quad \text{with} \quad \mathbf{d}_s = \underbrace{P_s \mathbf{d}_{1s}}_{\mathbf{d}_{Ns}} + \underbrace{(I - P_s) \mathbf{d}_{2s}}_{\mathbf{d}_{Os}} \quad (10)$$

The Jacobian null-space component  $\mathbf{d}_{Ns}$  is obtained as:

$$\begin{cases} \tau_s^T P_s \mathbf{d}_{1s} + w_s = 0 \\ g(\mathbf{d}_{1s}) = \frac{1}{2} \mathbf{d}_{1s}^T \mathbf{d}_{1s} \Rightarrow \underset{\mathbf{d}_{1s}}{\operatorname{argmin}} \{g(\mathbf{d}_{1s})\} \end{cases} \Rightarrow \mathbf{d}_{Ns} = \alpha_{Ns} P_s \tau_s$$

$$\text{with } \alpha_{Ns} = \begin{cases} \frac{-w_s}{\tau_s^T P_s \tau_s} & \text{if } \begin{cases} w_s < 0 \\ \tau_s^T P_s \tau_s > 0 \end{cases} \\ 0 & \text{otherwise} \end{cases} \quad (11)$$

where  $\alpha_{N_s}$  is the damping element of the controller in the  $N$  subspace and  $\boldsymbol{\tau}_s$  is the commanded slave torque. Since  $\mathbf{d}_{N_s}$  is a joint space velocity performed in the  $N$  subspace, the damping element can be limited on the base of the maximum displayable velocity in the  $N$  subspace in a certain moment:

$$\|\mathbf{d}_{N_s}\| \leq \|P_s \dot{\mathbf{q}}_{MAX_s}\| \Rightarrow \bar{\alpha}_{N_s} = \sqrt{\frac{\dot{\mathbf{q}}_{MAX_s}^T P_s \dot{\mathbf{q}}_{MAX_s}}{\boldsymbol{\tau}_s^T P_s \boldsymbol{\tau}_s}} \quad (12)$$

where  $\dot{\mathbf{q}}_{MAX_s}$  is the maximum joint speed vector and  $\bar{\alpha}_{N_s}$  is the  $N$  subspace maximum damping. The energy dissipated by this vector (up to its limit) is  $w_{N_s} = \alpha_{N_s} \boldsymbol{\tau}_s^T P_s \boldsymbol{\tau}_s$ . If  $|w_{N_s}| < |w_s|$  the residual power will be dissipated in the  $O$  subspace. Thus, the Jacobian null-space orthogonal component  $\mathbf{d}_{O_s}$  can be obtained as follows:

$$\begin{cases} \boldsymbol{\tau}_s^T (I - P_s) \mathbf{d}_{2_s} + (w_s + \bar{\alpha}_{N_s} \boldsymbol{\tau}_s^T P_s \boldsymbol{\tau}_s) = 0 \\ g(\mathbf{d}_{2_s}) = \frac{1}{2} \mathbf{d}_{2_s}^T \mathbf{d}_{2_s} \Rightarrow \underset{\mathbf{d}_{2_s}}{\operatorname{argmin}} \{g(\mathbf{d}_{2_s})\} \Rightarrow \mathbf{d}_{O_s} = \alpha_{O_s} (I - P_s) \boldsymbol{\tau}_s \end{cases}$$

with  $\alpha_{O_s} = \begin{cases} \frac{-(w_s + \bar{\alpha}_{N_s} \boldsymbol{\tau}_s^T P_s \boldsymbol{\tau}_s)}{\boldsymbol{\tau}_s^T (I - P_s) \boldsymbol{\tau}_s} & \text{if } \begin{cases} (w_s + \bar{\alpha}_{N_s} \boldsymbol{\tau}_s^T P_s \boldsymbol{\tau}_s) < 0 \\ \boldsymbol{\tau}_s^T (I - P_s) \boldsymbol{\tau}_s > 0 \end{cases} \\ 0 & \text{otherwise} \end{cases} \quad (13)$

where  $\alpha_{O_s}$  is the damping element of the controller in the  $O$  subspace. As in the previous case, the damping element can be limited on the base of the maximum displayable velocity in the  $O$  subspace in a certain moment:

$$\|\mathbf{d}_{O_s}\| \leq \|(I - P_s) \dot{\mathbf{q}}_{MAX_s}\| \Rightarrow \bar{\alpha}_{O_s} = \sqrt{\frac{\dot{\mathbf{q}}_{MAX_s}^T (I - P_s) \dot{\mathbf{q}}_{MAX_s}}{\boldsymbol{\tau}_s^T (I - P_s) \boldsymbol{\tau}_s}} \quad (14)$$

where  $\bar{\alpha}_{O_s}$  is the maximum  $O$  subspace damping. The energy dissipated by this vector (up to its limit) is  $w_{O_s} = \alpha_{O_s} \boldsymbol{\tau}_s^T (I - P_s) \boldsymbol{\tau}_s$ .

### B. Impedance-based Formulation

The impedance-based formulation is completely symmetrical to the admittance-based one substituting torques with joint velocities and vice versa. The privileged subspace is a joint subspace so that the torques produced in this subspace do not result in forces in the Cartesian space. It is well known that  $\mathbf{f} = Q \boldsymbol{\tau}$ , where  $Q = (JB^{-1}J^T)^{-1}JB^{-1}$  is the transpose Jacobian pseudo-inverse matrix weighted for the robot inertia matrix  $B$  [21]. Thus, the projector in the privileged subspace is then defined as follows:

$$P_m = I - J_m^T (J_m B_m^{-1} J_m^T)^{-1} J_m B_m^{-1} \quad (15)$$

where  $I \in \mathbb{R}^{n_m \times n_m}$  is the identity matrix. Note that, contrary to the admittance-based case, the projector is idempotent, but not symmetric. Thus, the orthogonal is defined as  $O : \operatorname{Imm}\{(I - P_m)^T\}$ .

### C. Final Remarks and Limitations

The concept of privileged dissipation in null space, originally proposed in [19], has been reformulated in the joint space and extended for manipulators in admittance configuration. Although the formulation is dealt with in the

joint space, no modifications to the  $PO$ s are required nor is kinematic symmetry between master and slave required. It has been clearly demonstrated that power-limited actuators require a space in which to dissipate the energy that cannot be dissipated in the privileged subspace. In addition, the power limits require that a maximum damping that can be performed by the PC is defined. The best space to complete the dissipation of residual energy was found to be the subspace orthogonal to the privileged subspace. This is true in general for a priority-based dissipation logic regardless of the space (Cartesian or at the joints) where the dissipation is performed, however it is a point not guaranteed in previous works that have dealt with the same topic in the *state-of-the-art*. This point is solved by the presented approach in both robot configurations. Since the damping element is a scalar value, it was chosen to impose a scalar constraint in order to easily come to a reasonable new damping limit. The proposed limitation aims to bind the maximum damping to the power limits of a manipulator in a specific subspace limiting the norm of the dissipation vector with the norm of the maximum action (torque for admittance configuration and joint speed for impedance configuration) performable in a certain subspace. This way of limiting the damping has pros and cons. This approach guarantees that the dissipating action is limited in norm, but it does not guarantee that all joints respect their limit at the same time: this means that a certain joint may exceed its limits. However, it presents the following advantages over other approaches:

- the damping limited through a norm allows keeping the joint references reasonably close to the limits. Conversely, the sample time based limit may produce references much higher than the power limits of the actuators (in fact, think of a situation in which the sampling time is high, but the power limits of the actuators are extremely low for construction reasons. In this situation the damping is not properly limited).
- the proposed limit does not require the solution of a  $QP$  online problem and provides a closed-form equation for the maximum damping with consequent advantages, in particular in robotic stand alone applications.

It should be noticed that each  $PC$  performs its action at reference level. Thus, if the reference exceeds the limits, the system will behave as in saturation for a certain period of time. However, the proposed limitation produces references that are reasonably close to the joint limits for short period of time. The proposed limitation could be modified to be more conservative: if the limit joint vector is characterized by low variance (which means that all joints have similar limits in torques or in joint velocities), the maximum damping can be divided by a factor  $1/\sqrt{n}$  (with  $n$  number of joints) to take into account the worst case scenario in which only one joint is moved. However, the proposed limitation could be ineffective if the limit joint vector of the manipulator is characterized by high variance (the joints differ significantly each other in torques or in joint velocities limits).

## IV. SIMULATION AND RESULTS

### A. Simulation

To test the performance of the *rPC*, a simulation of a *PF* teleoperation architecture was implemented in MATLAB Simulink using the Robotic System Toolbox. The simulation runs at 5 *KHz* and lasts 8 *s*. The architecture consists of a master and a slave manipulator, both are 4-DoFs planar robot manipulators (see figure 5). This choice was only due to simplicity because no kinematical symmetry between master and slave is required. The robot parameters were reported in table I. Moreover, all robots actuators are power limited ( $\dot{q}_{MAX} = \pi \text{ rad/s}$ ;  $\tau_{MAX} = 80 \text{ Nm}$ ). The slave performs a low-level joint *PD* position control while the master performs a low-level joint *P* torque control. All the controllers have been calibrated for the best performance. In the simulations, gravity has been neglected as being a planar problem. At high level, the slave accepts a Cartesian velocity reference from the master, while the master accepts a Cartesian force reference. The Cartesian target trajectory requires to follow a planar trajectory where the two linear coordinates *x* and *y* are imposed resulting in two redundancy DoFs. This trajectory is reported to a force reference for the master (and summed to the external force to obtain the complete reference) through an impedance ( $k_f$ ) to roughly represent a human moving a master in a real teleoperation scenario. The trajectory has been designed so that the slave manipulators contact a stiff wall. The wall stiffness was set to  $k_w = 10 \text{ N/mm}$  and the damping parameter was  $b_w = 2\zeta\sqrt{k_w}$  with  $\zeta = 0.7$ . To guarantee a good trajectory following and hard contact it was chosen  $k_f = 5 \text{ N/mm}$ . The velocity is sent to the slave robot through a forward communication delay and the force is sent back to the master through a backward communication delay. The simulated *PF* architecture has been tested in two time delay conditions: constant time delay of 300 *ms* per channel (600 *ms* round trip delay) and variable time delay. It was chosen to implement the variable time

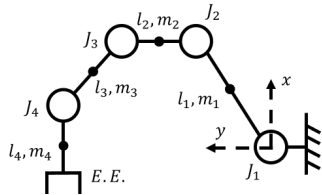


Fig. 5: Robot planar model for the simulation and Cartesian coordinates. Both the master and the slave manipulators of the *PF* architecture have the same kinematics for simplicity.

	$L_1$	$L_2$	$L_3$	$L_4$
$l$ [m]	0.25	0.25	0.25	0.25
$m$ [Kg]	1	1	1	1

TABLE I: Geometric and inertial parameters for the simulated manipulators. All the links were assumed to be cylindrical and with uniform mass distribution.

delay as a uniform pseudo-random number, which in the simulations can vary from 300 *ms* to 400 *ms* per-channel (up to 800 *ms* round trip delay). To guarantee stability, the simulated architecture has been passivated with the proposed *rPC* controllers. Moreover, to have comparison results, the same architecture in the same conditions has been passivated with the Multi-DoFs *PC* weighted with the Cartesian mass matrix. At least, a simulation has been conducted in which the master *PC* was implemented as in [19].

### B. Results

For the sake of conciseness, only the results of the simulation conducted under variable time delay will be presented. In fact, the results in the two delay conditions are comparable: even if the *cPC* appears noisier, the *rPC* is minimally influenced by the variable time delay. The results are reported in figure 6 limited to the *x* axis for clarity. To compare results at the end-effector level (which is the aim of this work), we projected both torque and joint velocity references of the *rPC* simulations at the Cartesian level. As expected, the stabilizing action of the *rPC* is much less evident at the Cartesian level with respect to the *cPC* one. The first row (plot (a-b)) shows the slave reference following the master and it is evident the better behaviour of the *rPC* controller. In particular, plot (e-f) report the Cartesian velocity reference among the passivated one. It is evident the better behaviour of the *rPC* controller. This result is confirmed by plot (c-d), in which the committed end-effector drift is computed as:

$$\mathbf{p}_{err}(k) = \Delta T \sum_{i=0}^k [\mathbf{v}_{sd}(i) - \hat{\mathbf{v}}_{sd}(i)] \quad (16)$$

It must be pointed out that in variable time delay condition, references that flow through a communication channel suffers from distortion phenomena [22]. Such a problem is also the source of unavoidable drift error both on the position and on the reference force. However, the drift reported in plot (c-d) are only due to the dissipating action and do not take into account the distortion phenomena (the speeds of equation 16 are measured after the delay and across the *PC*). The committed drift by the *rPC* approaches 1 *mm*, while the one committed by the *cPC* approaches 8 *cm*, which implies a worsening of almost 2 orders of magnitude with respect to the previous. Because slave manipulators drift in different ways, the wall position has been empirically adjusted to produce the same peak contact force. This ensures to have comparable force references at the master side. Plot (i-j) report the Cartesian reference force among the passivated one. Again, the behaviour of the *rPC* is obviously better. To better show this result, plot (g-h) report the difference between the impulse of the passivated force and the impulse of the non-passivated force over the same period of time (benchmark proposed in [23]). The impulse difference was computed as follows:

$$\mathbf{f}_{err}(k) = \Delta T \sum_{i=0}^k [\mathbf{f}_{md}(i) - \hat{\mathbf{f}}_{md}(i)] \quad (17)$$

Plot (i-j) also show that after a first hard strike, the feedback force reported to the master causes a move away



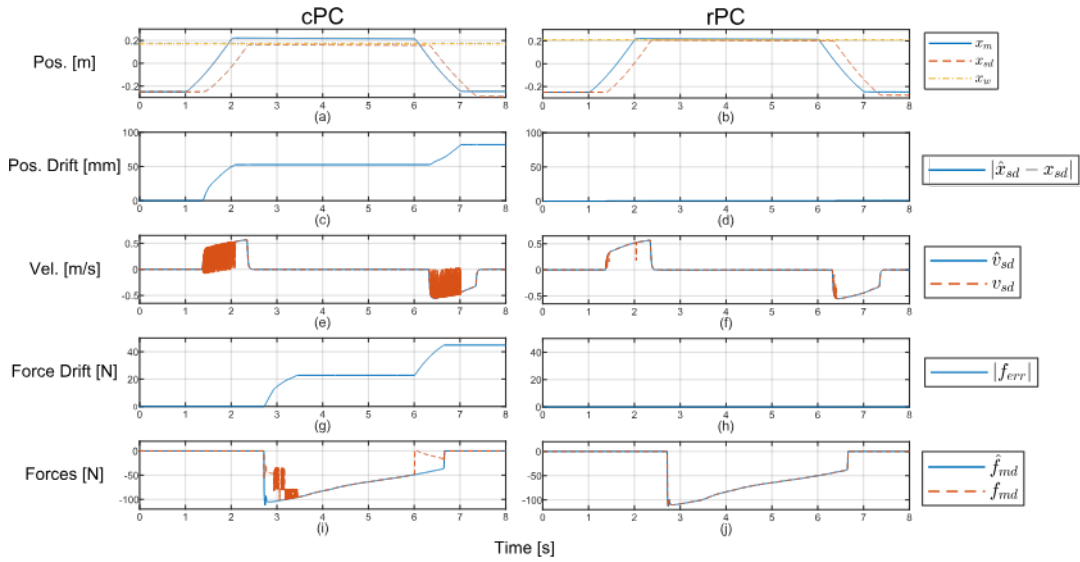


Fig. 6: The results of the simulation are divided into two columns, one per each *PC* implemented (*cPC* or *rPC*). Plot (a-b) show the master trajectory ( $\hat{x}_m$ ) and slave ( $x_{sd}$ ) x axis position, so as the wall position ( $x_w$ ). The drift errors are reported in plot (c-d), whereas the non-passivated ( $\hat{v}_{sd}$ ) and the passivated ( $v_{sd}$ ) velocities are shown in plot (e-f). Likewise, the impulse differences are reported in plot (g-h) and the non-passivated ( $\hat{f}_{md}$ ) and the passivated ( $f_{md}$ ) forces can be seen in plot (i-j).

from the wall. In fact, the force starts decreasing after the forward time delay passed and this can also be seen in a slight back deviation from the reference in plot (a-b) and plot (i-j). It should be noticed that the different positions of the wall, in accordance with different produced drift errors, produced the same peak forces making all the contacts comparable. In figure 7 the dissipation distribution between the privileged subspace and its orthogonal is reported both for master and slave. In particular, plot (a-b, e-f) report the actual damping among with its actual maximum computed as proposed respectively in the privileged subspace and in its orthogonal. It can be seen that in most of the cases this maximum damping is much lower than the one based on

the sampling time ( $\alpha_{MAX} = 1/(2T_c) = 2500$  1/s). In plot (c-d,g-h), the dissipating actions are reported respectively in the privileged subspace and in its orthogonal. It can be seen that the master is able to dissipate the overall energy in the null-space, while the slave requires a residual dissipation in the null-space orthogonal. However, the privileged strategy is evident with consequent benefits. The maximum damping in the admittance-based formulation appears to be noisier with respect the impedance-based case, this is probably the reason why the slave requires part of the dissipation in the task space. This noisy behaviour may depend on the nature of the commanded slave torques and may be solved by implementing a method symmetrical to the one proposed in [24]. As a further element of comparison, some of the results of the simulation performed by implementing the method proposed in [19] as master *PC* are reported in figure 8. The results for the slave have been omitted since, as there is no admittance formulation, the *cPC* has been implemented and it behaves identically as in the previous simulation. On the master side, the results are substantially identical to those obtained with the proposed *rPC* controller.

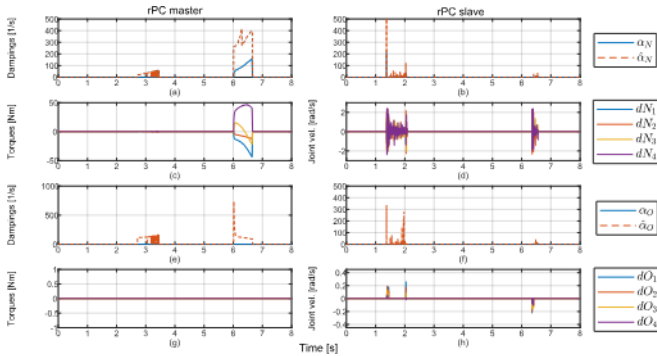


Fig. 7: *rPC* dissipation actions at joint level for master (right column) and slave (left column) manipulators. The first two rows refer to the  $N$  subspace dissipation, while the last two rows refer to the residual  $O$  subspace dissipation. Both damping (among with the computed maximum) and dissipation vectors were reported.

## V. DISCUSSIONS AND CONCLUSIONS

In this paper, a new joint level passivity controller formulation for both admittance-based and impedance-based kinematically redundant manipulators was proposed. This approach allows a privileged dissipation of the observed energy in the Jacobian null-space, guaranteeing the stability of the system at the best performance. It was shown that the best subspace where to dissipate the remaining observed energy is orthogonal to the privileged subspace. Moreover, the joint space formulation allowed for the definition of a maximum damping easily linked to the power limits of the actuators.

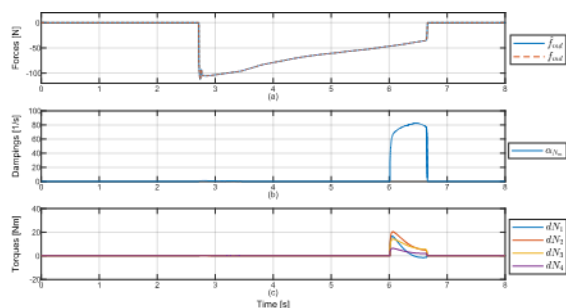


Fig. 8: Master  $PC$  behavior implemented as proposed in [19]. The end-effector force is untouched thanks to the  $N$  subspace dissipation. The damping limit ( $2500\ 1/s$ ) is never reached.

Even if this maximum damping has some limitations, it is a reasonable value with respect to common limits adopted in literature, with the advantage of a closed-form equation. Since references are still transmitted in the Cartesian domain, the proposed controller doesn't require any change in the  $POs$  and doesn't require kinematic symmetry between master and slave. The behaviour of the proposed controller was tested in simulation in presence of both constant and variable time delay. The simulation showed a strong improvement in performance compared to the  $cPC$  implementation both in terms of drift committed on the slave side and in terms of precision of the rendered force on the master side. Even if the  $cPC$  suffered more from the variable time delay condition, the  $rPC$  implementation showed similar performance to the constant time delay condition (neglecting the unavoidable distortion of the transmitted data). This means that the  $rPC$  greatly relieves both injected-energy-based drift compensation methods and rendered force enhancing methods under both constant and variable time delay conditions. In future works, the algorithm will be implemented on a real system among with a less conservatism TDPA formulation to improve system performance [25]. Moreover, it should be studied a method to improve the limitations related to the maximum damping proposed.

## REFERENCES

- [1] D. A. Lawrence, "Stability and transparency in bilateral teleoperation," in [1992] *Proceedings of the 31st IEEE Conference on Decision and Control*. IEEE, 1992, pp. 2649–2655.
- [2] K. Hashtrudi-Zaad and S. E. Salcudean, "Analysis of control architectures for teleoperation systems with impedance/admittance master and slave manipulators," *The International Journal of Robotics Research*, vol. 20, no. 6, pp. 419–445, 2001.
- [3] R. J. Anderson and M. W. Spong, "Bilateral control of teleoperators with time delay," in *Proceedings of the 1988 IEEE International Conference on Systems, Man, and Cybernetics*, vol. 1. IEEE, 1988, pp. 131–138.
- [4] G. Niemeyer and J.-J. Slotine, "Stable adaptive teleoperation," *IEEE Journal of oceanic engineering*, vol. 16, no. 1, pp. 152–162, 1991.
- [5] P. F. Hokayem and M. W. Spong, "Bilateral teleoperation: An historical survey," *Automatica*, vol. 42, no. 12, pp. 2035–2057, 2006.
- [6] B. Hannaford and J.-H. Ryu, "Time-domain passivity control of haptic interfaces," *IEEE transactions on Robotics and Automation*, vol. 18, no. 1, pp. 1–10, 2002.
- [7] J.-H. Ryu, Y. S. Kim, and B. Hannaford, "Sampled-and continuous-time passivity and stability of virtual environments," *IEEE Transactions on Robotics*, vol. 20, no. 4, pp. 772–776, 2004.
- [8] J. Artigas, J.-H. Ryu, C. Preusche, and G. Hirzinger, "Network representation and passivity of delayed teleoperation systems," in *2011 IEEE/RSJ International Conference on Intelligent Robots and Systems*. IEEE, 2011, pp. 177–183.
- [9] C. Preusche, G. Hirzinger, J.-H. Ryu, and B. Hannaford, "Time domain passivity control for 6 degrees of freedom haptic displays," in *Proceedings 2003 IEEE/RSJ International Conference on Intelligent Robots and Systems (IROS 2003)(Cat. No. 03CH37453)*, vol. 3. IEEE, 2003, pp. 2944–2949.
- [10] K. Hertkorn, T. Hulin, P. Kremer, C. Preusche, and G. Hirzinger, "Time domain passivity control for multi-degree of freedom haptic devices with time delay," in *2010 IEEE International Conference on Robotics and Automation*. IEEE, 2010, pp. 1313–1319.
- [11] X. Xu and E. Steinbach, "Elimination of cross-dimensional artifacts in the multi-dof time domain passivity approach for time-delayed teleoperation with haptic feedback," in *2019 IEEE World Haptics Conference (WHC)*. IEEE, 2019, pp. 223–228.
- [12] F. Porcini, D. Chiaradia, S. Marcheschi, M. Solazzi, and A. Frisoli, "Evaluation of an exoskeleton-based bimanual teleoperation architecture with independently passivated slave devices," in *2020 IEEE International Conference on Robotics and Automation (ICRA)*. IEEE, 2020, pp. 10205–10211.
- [13] J.-H. Ryu, J. Artigas, and C. Preusche, "A passive bilateral control scheme for a teleoperator with time-varying communication delay," *Mechatronics*, vol. 20, no. 7, pp. 812–823, 2010.
- [14] V. Chawda, H. Van Quang, M. K. O'Malley, and J.-H. Ryu, "Compensating position drift in time domain passivity approach based teleoperation," in *2014 IEEE Haptics Symposium (HAPTICS)*. IEEE, 2014, pp. 195–202.
- [15] H. Singh, A. Jafari, and J.-H. Ryu, "Enhancing the force transparency of time domain passivity approach: Observer-based gradient controller," in *2019 International Conference on Robotics and Automation (ICRA)*. IEEE, 2019, pp. 1583–1589.
- [16] T. Klamt, D. Rodriguez, L. Baccelliere, X. Chen, D. Chiaradia, T. Cichon, M. Gabardi, P. Guria, K. Holmquist, M. Kamedula *et al.*, "Flexible disaster response of tomorrow: Final presentation and evaluation of the centauro system," *IEEE robotics & automation magazine*, vol. 26, no. 4, pp. 59–72, 2019.
- [17] A. Coelho, H. Singh, T. Muskardin, R. Balachandran, and K. Kondak, "Smoother position-drift compensation for time domain passivity approach based teleoperation," in *2018 IEEE/RSJ International Conference on Intelligent Robots and Systems (IROS)*. IEEE, 2018, pp. 5525–5532.
- [18] A. Coelho, C. Ott, H. Singh, F. Lizarralde, and K. Kondak, "Multi-dof time domain passivity approach based drift compensation for telemanipulation," in *2019 19th International Conference on Advanced Robotics (ICAR)*. IEEE, 2019, pp. 695–701.
- [19] C. Ott, J. Artigas, and C. Preusche, "Subspace-oriented energy distribution for the time domain passivity approach," in *2011 IEEE/RSJ International Conference on Intelligent Robots and Systems*. IEEE, 2011, pp. 665–671.
- [20] A. Coelho, H. Singh, K. Kondak, and C. Ott, "Whole-body bilateral teleoperation of a redundant aerial manipulator," in *2020 IEEE International Conference on Robotics and Automation (ICRA)*. IEEE, 2020, pp. 9150–9156.
- [21] O. Khatib, "A unified approach for motion and force control of robot manipulators: The operational space formulation," *IEEE Journal on Robotics and Automation*, vol. 3, no. 1, pp. 43–53, 1987.
- [22] K. Kosuge, H. Murayama, and K. Takeo, "Bilateral feedback control of telemanipulators via computer network," in *Proceedings of IEEE/RSJ International Conference on Intelligent Robots and Systems. IROS'96*, vol. 3. IEEE, 1996, pp. 1380–1385.
- [23] R. Daniel and P. R. McAree, "Fundamental limits of performance for force reflecting teleoperation," *The international journal of robotics research*, vol. 17, no. 8, pp. 811–830, 1998.
- [24] J.-H. Ryu, B. Hannaford, D.-S. Kwon, and J.-H. Kim, "A simulation/experimental study of the noisy behavior of the time-domain passivity controller," *IEEE transactions on robotics*, vol. 21, no. 4, pp. 733–741, 2005.
- [25] M. Panzirsch, J.-H. Ryu, and M. Ferre, "Reducing the conservatism of the time domain passivity approach through consideration of energy reflection in delayed coupled network systems," *Mechatronics*, vol. 58, pp. 58–69, 2019.